

Non thermal emission in clusters of galaxies

M. Arnaud

Laboratoire AIM, DAPNIA/Service d'Astrophysique - CEA/DSM - CNRS - Université Paris Diderot, Bât. 709, CEA-Saclay, F-91191 Gif-sur- Yvette Cedex, France e-mail: monique.arnaud@cea.fr

Abstract. I briefly review our current knowledge of the non thermal emission from galaxy clusters and discuss future prospect with Simbol-X. Simbol-X will map the hard X-ray emission in clusters, determine its origin and disentangle the thermal and non-thermal components. Correlated with radio observations, the observation of the non-thermal X-ray emission, when confirmed, will allow to map both the magnetic field and the relativistic electron properties, key information to understand the origin and acceleration of relativistic particles in clusters and its impact on cluster evolution.

Key words. Cosmology: observations, (Cosmology:) large-scale structure of Universe, Galaxies: cluster: general, (Galaxies) Intergalactic medium, X-rays: galaxies: clusters, Radio continuum: general, Magnetic fields

1. Introduction

The main baryonic cluster component is a hot intergalactic gas, emitting in X-ray predominantly through thermal Bremsstrahlung (Fig. 1). This gas is heated at typical temperatures between 2 and 10 keV during the hierarchical cluster formation: continuous accretion of surrounding matters and merger between clusters generate shocks that heat the gas to the virial temperature. In addition, large-scale magnetic field ($B \sim 0.1 - 1 \mu\text{G}$) and relativistic electrons ($E \sim 1 - \text{few GeV}$) are present in the intergalactic medium, as revealed by diffuse synchrotron emission (radio halos and radio relics) observed in a fraction of galaxy clusters (Fig. 2 and Feretti, these proceedings). These relativistic electrons can interact with the CMB photons to give inverse Compton non-thermal X-ray radiation.

About 50 clusters with diffuse radio emission are presently known. All present evidence of recent merger events, suggesting that these events provide the energy source of the relativistic electrons. However, the origin of the relativistic particles and the acceleration processes are still poorly understood (Brunetti 2003, for a review). A major difficulty comes from the large size of the radio halos ($\sim \text{Mpc}$). The lifetime of the electrons responsible for the emission is very short ($\sim 10^8$ years), much shorter than the diffusion time. The electrons must thus have been (re-) accelerated, or generated recently, by a mechanism acting at cluster scale. Several processes have been proposed and it is possible that all of them are important. These include injection of relativistic electrons from AGN or galactic winds, acceleration out of the thermal pool and/or re-acceleration of low energy non-thermal electrons by shocks and/or turbulence induced dur-

Send offprint requests to: M. Arnaud

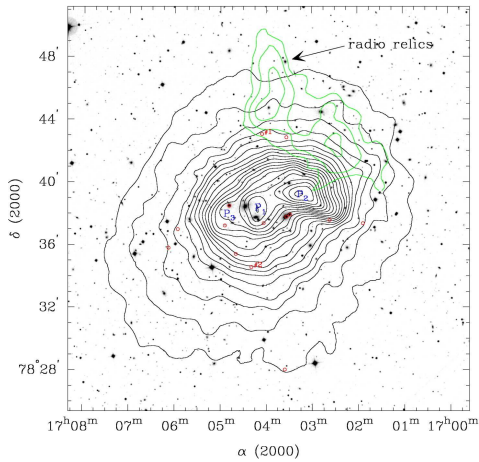


Fig. 1. Contours of the diffuse X-ray emission of A2256 as seen by *Chandra* (Sun et al. 2002)

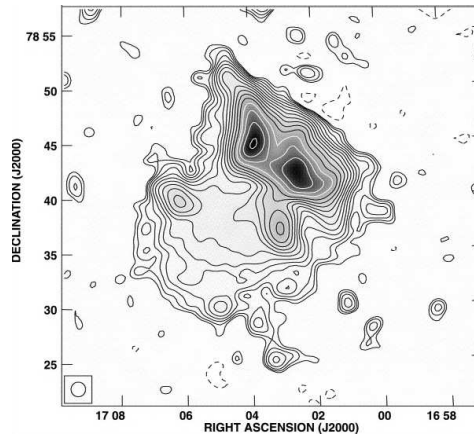


Fig. 2. VLA 1369 Mhz emission contours A2256 (Clarke & Ensslin 2006). Note the central radio halo and the peripheral radio relic (in the North).

ing merger events, continuous injection of secondary electrons by hadronic collisions of relativistic protons with the thermal gas. Similarly, the evolution of the intra-cluster magnetic field, from its primordial value, is poorly understood, although some recent numerical simulations now include it (e.g. Dolag 2002).

2. Radio and X-ray thermal emission

The density and energy distributions of the relativistic electrons, compared to that of the thermal electrons can help to distinguish between various models. For instance, a recent comparison of VLA radio maps and Chandra temperature maps of merging clusters suggest that radio halo electrons are mostly accelerated by turbulence rather than directly by shocks (Govoni et al. 2004). More stringent constraints are given by radio spectral index maps. Compared with X-ray data, they provided the first confirmation that cluster mergers do supply energy to the radio halo (Feretti et al. 2004). However, such data are presently available for only seven clusters (Giovannini et al. 1993; Feretti et al. 2004; Giacintucci, et al. 2005; Clarke & Ensslin 2006; Orrù et al. 2007)

Dramatic progresses in this field are expected with *LOFAR*, as it will allow for radio multi-frequency imaging with a typical two order of magnitude gain in sensitivity, at

a resolution similar to those of X-ray satellites. *LOFAR* should also detect ~ 1000 clusters (Cassano et al. 2006), of which 25% are expected to be at $z > 0.3$, a unique sample for statistical studies (frequency of radio halos, correlations between X-ray and radio properties...).

3. Hard X-ray emission

Radio observations provide important constraints on models, but not a full picture, the intensity of the synchrotron emission depending in a degenerate way on the strength of the magnetic field and on the relativistic electron density. The magnetic field can be estimated independently through Faraday rotation measure effects on the position angle of polarized emission from radio source viewed through the ICM (e.g. Govoni et al. 2006). However, the measure is limited, by nature, to a few lines of sight, i.e. this technique sparsely probes the cluster magnetic field, and parametric models of its spatial distribution have to be assumed.

On the other hand, the Inverse Compton (IC) X-ray emission only depends on the properties of the relativistic plasma. By combining its intensity to that of the radio emission, one can break the degeneracy on the magnetic field strength and estimate the density of the relativistic electrons. For a classical power-law electron spectrum, the

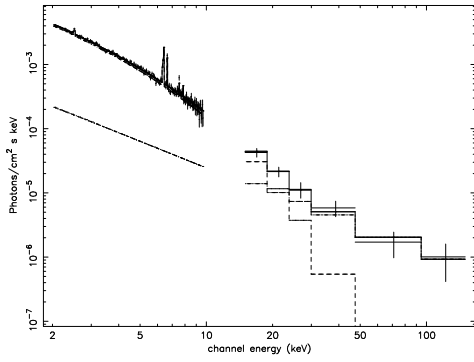


Fig. 3. Unfolded *Beppo-SAX* spectrum of A2256 (Fusco-Femiano et al. 2000). The dashed line is the thermal component ($kT \sim 7$ keV) and the dot-dashed line the non-thermal component ($\alpha = 1.4$).

spectrum of the IC emission is a power law. It is expected to dominate the thermal emission only at very low energy or beyond its exponential cut-off at high energy, i.e. typically above 10 keV (Fig. 3). A significant excess of emission at high energy, with respect to an isothermal emission model, has now been detected in 13 clusters with *Beppo-SAX* (Kaastra et al. 1999; Fusco-Femiano et al. 2003, 2005, 2007; Nevalainen et al. 2004) or *RXTE* (Gruber & Rephaeli 2002; Rephaeli & Gruber 2002, 2003; Petrosian et al. 2006; Rephaeli et al. 2006).

However, the significance of the excess is low ($< 5\sigma$) and still very sensitive to possible systematic errors on the background level (Rossetti & Molendi 2004; Fusco-Femiano et al. 2007). Furthermore, due to the lack of spatial information, the interpretation of the measured *global* spectrum is ambiguous. It is uncertain whether the excess is due to IC emission or an artifact of the complex multi-temperature plasma (Fig. 4) observed in non-relaxed clusters (e.g. Rephaeli & Gruber 2003, see also Renaud et al. 2006). Possible contamination by AGNs in the field of view is also an issue.

4. Measuring the cluster IC emission with *Simbol-X*

Thanks to its unique spectro-imaging capabilities up to high energies, *Simbol-X* will allow

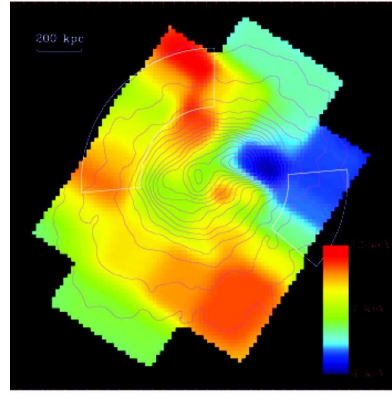


Fig. 4. Temperature map of A2256 measured with *Chandra* (Sun et al. 2002). X-ray emission isocontours are overlaid. Temperature ranges from 4 keV (blue) to 10 keV (red).

unambiguous study of the hard X-ray (HXR) emission from clusters. The AGNs contributions will be resolved and could be excised from the analysis. Spectra could be extracted in reasonably isothermal regions (or in regions of known thermal structure), allowing us to dis-

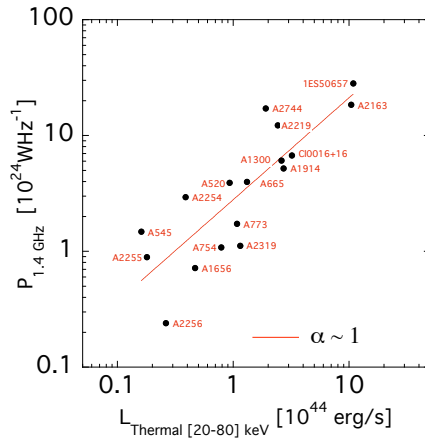


Fig. 5. Correlation between the radio power at 1.4 GHz and the thermal hard X-ray luminosity ([20–80] keV), for known clusters with giant radio halos. Data were derived from the compilation of Cassano et al. (2006). The dependence, $P_{\text{radio}} \propto L_{\text{THXR}}$, is found to be less steep than with the soft X-ray luminosity, $P_{\text{radio}} \propto L_{\text{TSXR}}^2$ (Cassano et al. 2006), because the temperature increases with luminosity and thus the $L_{\text{THXR}}/L_{\text{TSXR}}$ ratio.

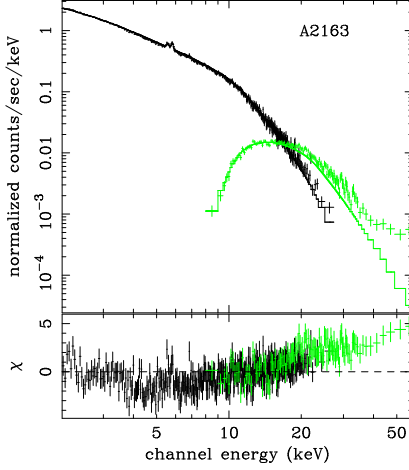
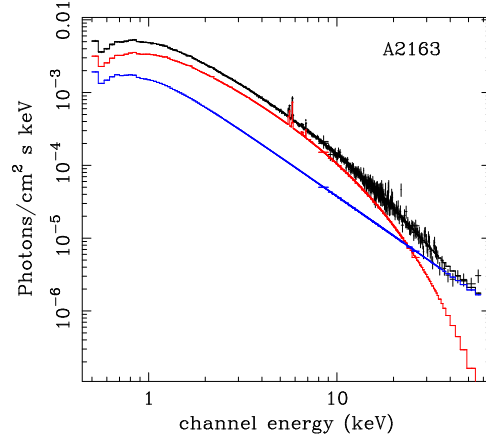
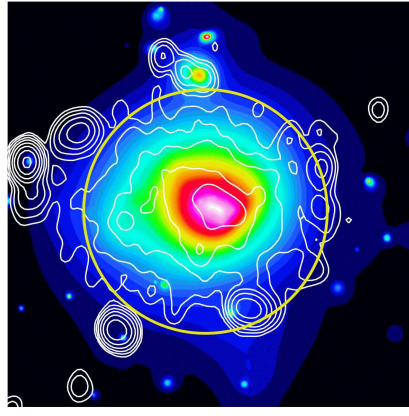


Fig. 6. Simulated *Simbol-X* spectrum of A2163 ($z=0.2$) for a 150 ksec exposure time. *Top-left panel:* *XMM-Newton* image with radio contours (Feretti et al. 2001) overlaid. The circle corresponds to the *Simbol-X* FOV (11' diameter). *Top-right panel:* Unfolded spectrum integrated over the whole FOV. Red line: thermal component estimated from *XMM-Newton* data (mean $kT = 12$ keV). Blue line: IC component, as estimated by Rephaeli et al. (2006) with *RXTE* ($S_{IC,[20-80] \text{ keV}} = 1.1 \cdot 10^{-11} \text{ ergs/s/cm}^2$, power law index of $\alpha = 1.8$). The slope and normalisation are measured with an accuracy of $\pm 2\%$ and $\pm 8\%$, respectively. *Bottom-left panel:* Observed spectrum with the MPD (black) and with the CZT (green) detectors. The line is the best fit isothermal model. The excess at high energy due to the IC emission is clearly detected at the 21σ confidence level, allowing its mapping (e.g. ~ 16 sub-regions at 5σ detection level).

entangle the thermal and non-thermal components.

The IC flux scales with the radio flux, redshift and magnetic field B , as :

$$S_{IC} \propto S_{radio}(z+1)^{2+\alpha} B^{-\alpha} \quad \text{with } \alpha \sim 2. \quad (1)$$

Obviously the IC emission will be easier to detect in clusters with bright radio halos. The radio luminosity steeply increases with the thermal *soft* X-ray luminosity, $P_{radio} \propto L_{TSXR}^2$ (Cassano et al. 2006), but only as $P_{radio} \propto L_{THXR}$ with the thermal *hard* X-ray luminosity (see Fig. 5). In practice, for a given B value, the thermal HXR flux will be proportional to the IC flux, and the detection of the IC emission

over the thermal HXR emission will never be easy. One can however take advantage of the different redshift dependence of the IC and radio/thermal X-ray emission, by choosing the highest z cluster for a given radio flux (Eq. 1).

Promising *Simbol-X* targets are thus clusters with bright radio halos at intermediate redshift ($z \sim 0.2$). Furthermore, at these redshifts, the cluster size well matches the FOV of *Simbol-X* (Fig. 6 top panel). An example is A2163 (Fig. 6), a massive cluster undergoing major merger event, which host the brightest radio halo known so far, and for which HXR excess have indeed been detected. Note that the *LOFAR* survey will make a complete census of

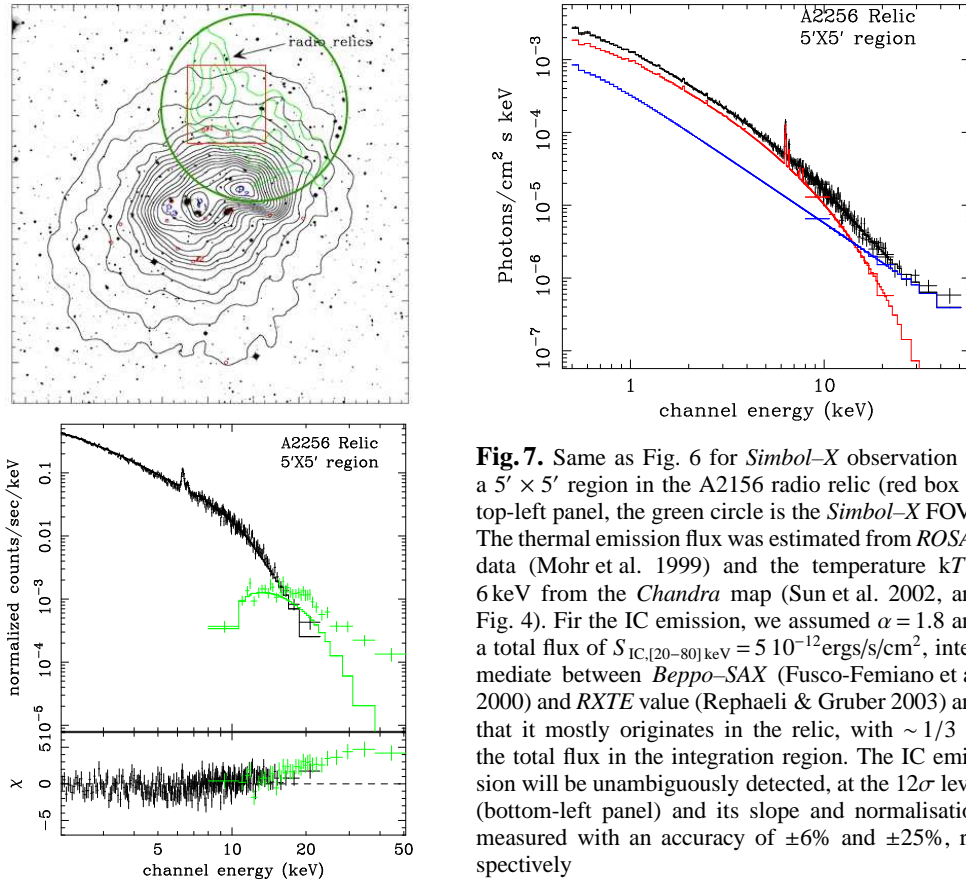


Fig. 7. Same as Fig. 6 for *Simbol-X* observation of a $5' \times 5'$ region in the A2156 radio relic (red box in top-left panel, the green circle is the *Simbol-X* FOV). The thermal emission flux was estimated from *ROSAT* data (Mohr et al. 1999) and the temperature $kT = 6$ keV from the *Chandra* map (Sun et al. 2002, and Fig. 4). For the IC emission, we assumed $\alpha = 1.8$ and a total flux of $S_{\text{IC}, [20-80] \text{ keV}} = 5 \cdot 10^{-12} \text{ ergs/s/cm}^2$, intermediate between *Beppo-SAX* (Fusco-Femiano et al. 2000) and *RXTE* value (Rephaeli & Gruber 2003) and that it mostly originates in the relic, with $\sim 1/3$ of the total flux in the integration region. The IC emission will be unambiguously detected, at the 12σ level (bottom-left panel) and its slope and normalisation measured with an accuracy of $\pm 6\%$ and $\pm 25\%$, respectively

clusters with bright radio halos and is expected to provide ~ 100 suitable targets for *Simbol-X* (Brunetti, these proceedings). *Simbol-X* will also be particularly powerful for the study of the IC emission in radio relics, located at the cluster periphery, the thermal emission decreasing with radius (Fig. 7).

Simbol-X will easily detect IC emission at the level reported by *Beppo-SAX* or *RXTE*, $S_X \sim 10^{-11} \text{ cgs}$ in the $[20-80] \text{ keV}$ energy band, with a much improved signal to noise ratio (Fig. 6 and Fig 7). However, the IC flux expected for a given radio flux is very uncertain, due to uncertainties in the magnetic field intensity (Eq. 1). It must be noted that estimates of the magnetic field value from the *Beppo-SAX* or *RXTE* observations of the HXR excess, assumed to be IC emission,

are up to on order of magnitude lower than that estimated through Faraday depolarisation and the actual IC flux could be significantly smaller than the values quoted above. Recent theoretical attempts significantly reduced the discrepancy, though, (Brunetti et al. 2004; Colafrancesco et al. 2005), assuming that the magnetic field decreases towards the cluster outskirts. In any case, *Simbol-X* measurements, combined with radio synchrotron observations, will provide tight independent lower limits on the B value, if the IC emission is not detected, and a firm characterisation, if it is detected at the level of previous observations.

The intensity of the IC emission, when confirmed, will constrain the density of the relativistic electrons. Its spectral index, measured

with high precision (Fig. 6 and Fig. 7) will constrain the electron spectrum, complementary to the constraints provided by the radio spectrum. These measurements, giving clean access to the energetics of the relativistic particles, will be invaluable to distinguish between models. Comparison between the density and energy spatial distribution of the relativistic electrons and the ICM temperature structure will provide further information on the acceleration process (e.g. via shocks or turbulence).

The study on non thermal emission with *Simbol-X* has further cosmological implications. A better understanding of relativistic particles in clusters will provide new insights on the cluster formation process, e.g. how the energy released during merger events is redistributed between the thermal and non-thermal components. The non thermal ICM pressure will be estimated, allowing us to assess potential errors currently made when estimating total cluster mass (a key quantity when using clusters to constrain cosmological parameters) from X-ray observations and the hydrostatic equilibrium equation.

5. Conclusions

Major progresses on the IC emission in cluster are expected with *Simbol-X*. Combined with new generation radio observations, e.g. with *LOFAR*, *Simbol-X* will provide key diagnostics on the origin and acceleration of relativistic particles in clusters and its impact on cluster evolution. The science that will be done by *Simbol-X* should also benefit from *GLAST*, which will provide additional information on the protons population, and on high energy electrons accelerated at merger and accretion shocks.

References

- Brunetti, G., 2003, in *Matter and Energy in Clusters of Galaxies*, ASP Conf. Ser., ed. S. Bowyer & C.-Y. Hwang, 301, 349
- Brunetti, G., Blasi, P., Cassano, R. & Gabici, S., 2004, *MNRAS*, 350, 1174
- Clarke, T.E. & Ensslin, T.A. 2006, *AJ*, 131, 2900
- Colafrancesco, S., Marchegiani, P. & Perola, G.C. 2005, *A&A*, 443, 1
- Cassano, R., Brunetti, G. & Setti, G. 2006, *MNRAS*, 369, 1577
- Dolag, K., Bartelmann, M. & Lesch, H. 2002, *A&A*, 387, 383
- Feretti, L., Fusco-Femiano, R., Giovannini, G. & Govoni, F. 2001, *A&A*, 373, 106
- Feretti, L., Orrù, E., Brunetti, G. et al. 2004, *A&A*, 423, 111
- Fusco-Femiano, R., Dal Fiume, D., De Grandi, S. et al. 2000, *ApJ*, 534, L7
- Fusco-Femiano, R., Orlandini, M., De Grandi, S. et al. 2003, *A&A*, 398, 441
- Fusco-Femiano, R., Orlandini, M., Brunetti, G. et al. 2004, *ApJ*, 602, L73
- Fusco-Femiano, R., Landi, R. & Orlandini, M. 2005, *ApJ*, 624, L69
- Fusco-Femiano, R., Landi, R. & Orlandini, M. 2007, *ApJ*, 654, L9
- Giacintucci, S., Venturi, T., Brunetti, G. et al. 2005, *A&A*, 440, 867
- Giovannini, G., Feretti, L., Venturi, T. et al. 1993, *ApJ*, 406, 399
- Govoni, F., Markevitch, M., Vikhlinin, A. et al. 2004, *ApJ*, 605, 695
- Govoni, F., Murgia, M., Feretti, L. et al. 2006, *A&A*, 460, 425
- Gruber, D., & Rephaeli, Y. 2002, *ApJ*, 565, 877
- Kaastra, J., Lieu, R., Mittaz, P.D. et al., 1999, *ApJ*, 519, L119
- Mohr, J., Mathiesen, B. & Evrard, A. 1999, *ApJ*, 517, 627
- Nevalainen, J., Oosterbroek, T., Bonamente, M. & Colafrancesco, S. 2004, *ApJ*, 608, 166
- Orrù, E., Murgia, M., Feretti, L. et al. 2007, *A&A*, 467, 943
- Petrosian V., Madejski, G. & Luli, K. 2006, *ApJ*, 652, 948
- Renaud, M., Bélanger, G., Paul, J., Lebrun, F., Terrier, R. 2006, *A&A*, 453, L5
- Rephaeli, Y., & Gruber, D. 2002, *ApJ*, 579, 587
- Rephaeli, Y. & Gruber, D. 2003, *ApJ*, 595, 137
- Rephaeli, Y., Gruber, D. & Arieli, Y. 2006, *ApJ*, 649, 677
- Rossetti, M. & Molendi, S. 2004, *A&A*, 414, L41
- Sun, M., Murray, S.S., Markevitch, M. et al. 2002, *ApJ*, 565, 867